Optically splitting symmetric neuron pairs in *C. elegans*

Lloyd Davis[1], Inja Radman[2]*, Angeliki Goutou[1]*, Ailish Tynan[1], Kieran Baxter[1], Zhiyan Xi[1], Jason W. Chin[2], Sebastian Greiss[1,3]

[1] Centre for Discovery Brain Sciences, University of Edinburgh, UK
[2] Medical Research Council Laboratory of Molecular Biology, Cambridge, UK
* These authors contributed equally
[3] s.greiss@ed.ac.uk

Abstract

Two thirds of the 302 neurons in *C. elegans* form bilaterally symmetric pairs in its physical connectome, and similar gross morphological symmetries are seen in the nervous systems of many other animals. A central question is whether and how this morphological symmetry is broken to produce functional asymmetry. Addressing this question, in all but two cases, has been impossible because no promoters are known that can direct gene expression to a single cell within a symmetric pair. Here we develop an efficient genetic code expansion system in *C. elegans* and use this system to create a photo-activatable version of Cre recombinase. Using this system, we target single neurons within a bilaterally symmetric pair (PLMR and PLML) with a laser. This turns on Cre and thereby switches on expression of an optogenetic channel in a single cell. We hereby overcome the limitation that these neurons cannot be targeted by genetic means. Our approach enables the generation of large numbers of animals for downstream experiments. By globally illuminating groups of freely moving animals to stimulate the targeted neurons that express an optogenetic channel we dissect the individual contributions of PLMR and PLML to the *C. elegans* touch response. Our results reveal that the individual neurons make asymmetric contributions to this behaviour, and suggest distinct roles for PLMR and PLML in the habituation to repeated stimulation. Our results demonstrate how genetic code expansion and optical targeting can be combined to break the symmetry of neuron pairs in *C. elegans* and thereby dissect the contributions of individual neurons to behaviour.

Introduction

Defining the molecular and cellular basis of behavior is a fundamental challenge in neuroscience. *C. elegans* contains 302 neurons, for which the physical connectivity has been determined[1]. This physical map provides a conceptual framework within which to design experiments to understand the signal processing properties of the neural circuits that define behavior. Central to this endeavor are methods for the spatiotemporal control of gene expression that enable precise perturbations to be effected in individual cells or collections of cells and thereby advance our understanding of cellular contributions to circuit function. Two thirds of the neurons in *C. elegans* exist in bilaterally symmetric (left and right) pairs, and similar gross morphological symmetries are seen in the nervous systems of many other animals. A central question is whether and how this morphological symmetry is broken to produce functional asymmetry[2–5]. General strategies to control gene expression in single cells would provide an approach to address this question and many other fundamental questions in biology.

Tissue specific promoters (or their combination) can be used to target some groups of cells, but this approach offers only limited precision, and in many cases appropriate promoters are not available; this is especially true when investigators aim to limit expression to only a single cell or a defined subset of cells. With two notable exceptions (the ASE and AWC sensory neuron pairs)[5] tissue specific promoters or not available that target individual neurons within a symmetric pair. Laser ablation allows the removal of specific neurons, but does not allow the study of intact circuits. The behavioral outputs of groups of cells in *C. elegans* has been controlled optogenetically by optical tracking to spatially limit the region of the worm that is illuminated[6,7], but this approach in most cases does not have the spatial precision to target single cells. Moreover, since worms move on their sides, individual neurons within bilaterally symmetric pairs cannot be targeted in a moving animal. In limited cases targeting gene expression to individual cells has been demonstrated through the use of a pulsed infrared laser to selectively induce heat-shock only in single cells[8,9]. However, this approach is both technically challenging and labour intensive, severely limiting its potential for widespread application; furthermore, this approach has not been used to target single neurons within a symmetric pair.

Sequence specific DNA recombinases, such as Cre and FLP, are widely used to control gene expression in many systems – including worms, flies, and vertebrates. They can be used to irreversibly either activate or deactivate the expression of target genes. We envisioned that the creation of an optically activated recombinase in *C. elegans* might enable the optical targeting of gene expression to single cells. The photo-induced reconstitution of split recombinases[10,11] might be used to optically target recombinase activity to a single cell. However, this approach has not been

employed in *C. elegans*, and may be hampered by high background levels of light independent recombinase activity. Moreover, these systems are induced using blue light, making their use incompatible with most optogenetic and imaging applications and requiring cells to be kept in the dark, making their use in transparent systems, such as *C. elegans* difficult. Recently, genetic code expansion[12] was used to create photo-caged versions of Cre in cultured mammalian cells and Zebrafish embryos[13,14]. In this approach, an orthogonal aminoacyl-tRNA synthetase (aaRS) / $tRNA_{CUA}$ pair is used to direct the site-specific co-translational incorporation of a photocaged tyrosine or lysine residue in place of a catalytically critical lysine or tyrosine residue in the active site of Cre. This results in a catalytically inactive enzyme[13,14]. The photo-caging group can then be removed through a short exposure to 365 nm UV light, thereby activating Cre recombinase, which in turn activates expression of its target genes. Since *C. elegans* was the first multicellular organism in which genetic code expansion was established and the incorporation of non-canonical amino acids (ncAA) is possible in all *C. elegans* tissues[15] we decided to create a photocaged Cre system in C. elegans to enable the optical activation of gene expression in single cells.

Here we describe the optimization of genetic code expansion for ncAA incorporation and the optimization of a photo-caged Cre recombinase variant (optPC-Cre) in *C. elegans*. The combination of these advances allows us to go from a system in which we can optically control gene expression in less than 1% of animals to an optimized system in which we can optically activate gene expression in more than 95% of animals in the population. This enables downstream studies of behavior. By using a microscope mounted 365 nm laser we photo-activate Cre and thereby control gene expression in single cells. We name this approach **Laser Targeted Activation of Cre-Lox recombination** (Laser-TAC). Laser-TAC is fast and within the technical capabilities of any lab currently able to perform laser ablation, allowing easy generation, in a single session, of dozens of animals with defined expression patterns for use in downstream experiments. We demonstrate the utility of Laser-TAC by using it to target the expression of optogenetic channels to individual *C. elegans* touch sensory neurons within a left/right pair (PLML and PLMR). These individual neurons cannot be targeted by other methods, and our approach allows us to study their contribution behavior for the first time. Our results reveal that the individual neurons within this pair make an asymmetric contribution to the touch response, and suggest distinct roles for PLMR and PLML in the habituation to repeated stimulation.

Results

Improved ncAA incorporation

Efficient genetic code expansion depends on the ability of the orthogonal aminoacyl tRNA synthetase to aminoacylate its cognate $tRNA_{CUA}$, which in turn delivers the ncAA to the ribosome for incorporation in response to an amber stop codon (**Fig. 1**). As the charging of the ncAA onto the $tRNA_{CUA}$ is a largely cytoplasmic occurrence, the efficiency of this charging is dependent on the availability of the PylRS in the cytoplasm.

The archean *Methanosarcina mazei* PylRS is localised predominantly to the nucleus, due to a stretch of positively charged amino acids in the N-terminal domain, which act as a nuclear localisation sequence in eukaryotes. The addition of a rationally designed strong nuclear export sequence (S-NES) to the N-terminus of PylRS has been shown to significantly increase incorporation efficiency of ncAA in mammalian cell culture by increasing the amount of cytoplasmic PylRS[16].

To improve incorporation efficiency in *C. elegans* we decided to test this approach by adding the S-NES sequence to the N-terminus of PCKRS, a PylRS variant optimised for the incorporation of a photo-caged lysine (PCK)[17] (**Fig. 2a**). We expressed S-NES::PCKRS using the ubiquitous P*sur-5* promoter[18], while the $tRNA(Pyl)_{CUA}$ was expressed from the ubiquitously active P*rpr-1* promoter[19]. To assay incorporation efficiency of PCK we used a dual color incorporation sensor, consisting of a ubiquitously expressed GFP::mCherry fusion, with the two proteins separated by an amber stop codon[15] (**Fig. 2b**).

To our surprise we could detect no significant difference in incorporation between animals expressing unmodified PCKRS and S-NES::PCKRS. In fact, incorporation levels using the S-NES::PCKRS construct appeared to be even lower than using unmodified PCKRS (**Fig. 2c**). To test whether S-NES::PCKRS and unmodified PCKRS indeed localize as predicted in *C. elegans*, we expressed both S-NES::PCKRS::GFP and PCKRS::GFP fusion proteins. We found that while unmodified PCKRS::GFP was almost entirely nuclear, the S-NES::PCKRS::GFP fusion localized to the cytoplasm, showing that the S-NES did in fact efficiently shift localisation of PCKRS from the nucleus to the cytoplasm (**Fig. 2d**). We suspected that the S-NES tag might impinge on the functionality of PCKRS in *C. elegans*. We therefore performed a mini-screen of additional NESs, derived from human proteins which have been demonstrated to act as NESs in *C. elegans*: p120cts NES, PKIα NES, and Smad4 NES[20]. Indeed, we found that all tested NES sequences result in successful export of PCKRS from the nucleus (**Fig. 2d**). When we co-expressed PCKRS variants containing these NESs with tRNA(Pyl) and the GFP::mCherry incorporation reporter, we found that whereas p120cts NES appeared to reduce incorporation efficiency below the level of unmodified PCKRS, the two other NESs, the PKIα NES and the Smad4 NES, markedly increased incorporation efficiency of PCK (**Fig. 2c**). We chose these two most efficient PCKRS variants for subsequent

optimisation experiments.

It has been shown that tRNA(Pyl) represents a further limiting factor for ncAA incorporation in mammalian cells, likely due to a secondary structure that is significantly divergent from that of canonical mammalian tRNAs resulting in a low level of compatibility with the endogenous translational machinery. Introducing elements of mammalian tRNAs into the archeal tRNA(Pyl), or conversely introducing identity elements required for recognition of tRNA(Pyl) by PylRS into a bovine mitochondrial tRNA was reported to improve ncAA incorporation efficiency in mammalian cell culture[21].

In order to investigate whether the same might hold true for other eukaryotes, we decided to test an improved tRNA variant in the *C. elegans* system. We co-expressed Smad-4-NES::PCKRS and PKIα -NES::PCKRS with previously reported bovine mitochondrial tRNA based variant C15[21] in *C. elegans* together with the GFP::mCherry incorporation reporter. We found that replacement of tRNA(Pyl) with tRNA(C15), further increased incorporation efficiency (**Fig. 2c,e,f,g).** Compared to the unmodified PCKRS / tRNA(Pyl) pair, the Smad-4-NES::PCKRS / tRNA(C15) and PKIa-NES::PCKRS / tRNA(C15) pairs both improved incorporation efficiencies more than 50 fold, from < 0.1% to between 4% - 5% (**Fig. 2f**). We performed all further experiments using the Smad4-NES::PCKRS / tRNA(C15) pair.

Expression of photo-caged Cre recombinase

We then applied our improved incorporation system in order to express photo-caged Cre recombinase (PC-Cre) in the N2 wild type laboratory strain of *C. elegans*. Cre recombinase can be photocaged by replacing K201, a lysine residue in the Cre active site, critical for enzyme activity, with photo-caged lysine (PCK)[14,22] (**Fig. 3a,b**).

PC-Cre has been expressed previously in both mammalian cell culture and zebrafish embryos, using transient transfection and direct mRNA/tRNA injections[13,14].

We replaced the lysine codon at position 201 with an amber stop codon to direct incorporation of PCK and generated transgenic lines expressing PCKRS, tRNA(Pyl) and PC-Cre(K201am) together with a Cre recombinase target gene, a fluorescently tagged channelrhodopsin ChR2::mKate2 separated from its promoter by a transcriptional terminator flanked by loxP sites. The PC-Cre construct was expressed in an artificial operon with GFP allowing us to visualize expression of the PC-Cre construct (**Fig. 3c**). We initially based the PC-Cre construct on previously reported Cre constructs, which contain an N-terminal SV40 NLS in addition to the internal NLS native to Cre[13,14,23,24], thus ensuring localisation of the enzyme to the nucleus.

We generated transgenic animals expressing all genetic components behind a *glr-1* promoter, an ortholog of human GRIA1 (glutamate ionotropic receptor AMPA type subunit 1), which is active in glutamatergic neurons, including the command interneurons[25] (**Supplementary Figure 1**). We grew the animals on PCK from the

L1 larval stage and activated PC-Cre by UV illumination after two days, when they had reached the L4 larval stage. We saw strong expression of ChR2::mKate2 in neurons expressing PC-Cre 24h after activation. In animals which had undergone UV illumination without prior feeding on PCK and in animals fed on PCK, but which had not undergone UV illumination we saw no expression of ChR2::mKate2 (**Supplementary Fig. 2**). Furthermore, as expected for a membrane channel, the red fluorescence of ChR2::mKate2 was localised at the cellular membrane. We observed red fluorescence only in cells expressing the P*glr-1* promoter, as evidenced by the overlap with P*glr-1* driven expression of GFP.

Using the optimised Smad4-NES::PCKRS / tRNA(C15) expression system, we observed expression of the target locus, indicative of PC-Cre photo-activation, in 63% of animals 24h after uncaging. We saw no red fluorescence without UV treatment. The 63% activation rate was a vast improvement compared to 1% observed with unmodified PCKRS and tRNA(Pyl) (**Fig. 3d**).

Improving photo-caged Cre Recombinase

To further improve the photo-activation method we next turned to the optimisation of PC-Cre. When using amber stop codons for ncAA incorporation, the $tRNA_{CUA}$ competes with endogenous release factors, resulting in a mixture of full length, ncAA containing, incorporation product, and truncated product due to translational termination at the amber stop codon. Using the GFP::mCherry incorporation reporter we show that the percentage of full-length product when using the improved Smad-4-NES::PCKRS / tRNA(C15) incorporation system is between 4% - 5% (**Fig. 2f**).

Whilst a Cre protein truncated at the amber stop codon in position 201 is missing the majority of its active site, the polypeptide responsible for the protein-protein interaction interface involved in forming active Cre tetramers is still present, as are large parts of the DNA binding interface. We therefore cannot exclude the possibility that truncated Cre which is translocated to the nucleus due to the NLSs upstream of position 201 may interfere with tetramer formation or DNA binding of the tetramer[26].

Since Cre acts on nuclear DNA, we hypothesised that we could boost PC-Cre activity by lowering the fraction of truncated PC-Cre while increasing the fraction of full-length PC-Cre present in the nucleus.

We therefore decided to remove both NLSs upstream of position 201 in the PC-Cre construct by introducing a R119A mutation disabling the internal NLS sequence and removing the N-terminal SV40 NLS. To restore nuclear import for full length PC-Cre only, we attached the strong *C. elegans egl-13* NLS[27] to the Cre C-terminus to create optimised PC-Cre (optPC-Cre) **(Fig. 3e)**. We thus aimed to utilise the *C. elegans* nuclear translocation machinery to enrich full-length product in the nucleus. When we compared optPC-Cre to PC-Cre, we observed a significant improvement of target gene activation from 63% for PC-Cre to 93% for optPC-Cre (**Fig. 3d**). We saw no expression of the ChR2::mKate2 target gene without PCK or UV activation **(Fig. 3f).**

We next performed behavioural assays to verify that using optPC-Cre to express

ChR2::mKate2 fusion protein resulted in neurons that could be optically controlled.

After activation of optPC-Cre we allowed 24h for sufficient expression of ChR2::mKate2, which we confirmed by visual inspection under a dissecting fluorescence microscope. When we then exposed worms to 470nm blue light to activate ChR2, we observed reversals in worms expressing ChR2::mKate2 in the presence of the ChR2 cofactor ATR, but no reaction in animals expressing ChR2::mKate2 in the absence of ATR **(Supplementary Videos 1,2)**. Our results concur with previous studies showing that optogenetic activation of neurons expressing ChR2 behind P*glr-1* induces backward movement[28]. We therefore concluded that optPC-Cre is a suitable tool to control expression of optogenetic channels for the purpose of optical control of neuronal activity.

Cell-specific Uncaging and Behaviour

Using light to control activity of Cre recombinase allows precise spatial control of Cre dependent DNA recombination. We decided to test the precision of uncaging by using a microscope mounted UV laser to target 365nm light to individual cells in the animal. For this we chose the posterior pair of touch sensory neurons PLML and PLMR.

C. elegans has six main mechanosensory neurons, of which AVM, ALML and ALMR are located in the anterior of the worm, whereas neurons PVM, PLML and PLMR are located in the posterior (**Fig. 4a**). Activation of the touch receptor neurons results in avoidance behavior which manifests in either forward or reverse movement, away from the stimulus[29]. Previous studies using targeted illumination of ChR2 in individual animals showed that optogenetic activation of the anterior neurons AVM and ALM results in reversals, while activation of the posterior neurons PVM and PLM results in a bias towards forward movement. Concurrent activation of all 6 neurons results in reversals in the majority of cases. Repeated activation leads to a reduced response due to habituation[6,7,30].

We decided to more closely investigate the PLM neuron pair, since the individual neurons of the pair show a striking asymmetry in their connections within the connectome (**Fig. 4b**). PLMR forms chemical synapses with 10 downstream neurons including the AVA and AVD interneuron pairs, which are involved in driving backward locomotion. In addition to chemical synapses PLMR also forms gap junctions to PVCR, PHCR, LUAR. PLML on the other hand is connected to the PVCL, PHCL, LUAL interneurons of the touch response circuit exclusively through gap junctions and does not form any chemical synapses with the exception of a single synapse to HSNL, a neuron involved in the control of egg laying[29]. Previous studies indicate that the asymmetric wiring of PLML and PLMR has functional relevance in the tap response, as ablating PLMR increases the animals backward movement in response to tap stimuli similar to the ablation of both PLM neurons, while ablating PLML has no effect[31].

We decided to investigate the contribution of individual PLM neurons to the tail touch response by selectively expressing the optogenetic channel Chrimson[30] in

either both PLML and PLMR together, or in PLML and PLMR individually. To this end we generated strains expressing Smad-4-NES::PCKRS and optPC-Cre behind a P *mec-7* promoter, which is active in all six mechanosensory neurons[32]. To express Chrimson we used a Chrimson::mKate2 fusion gene separated from the pan-neuronal P*maco-1* promoter by a transcriptional terminator flanked by loxP sites. We chose P*maco-1*, the promoter of *maco-1*, an ortholog of human MACO1 (macoilin 1)[33], because of its sustained expression in the nervous system during adulthood (**Supplementary Figure 1, Supplementary Figure 3**).

We grew age synchronised animals on PCK for two days from L1 onwards. At the L4 stage we mounted the animals on a microscope slide and used a Micropoint Galvo system to deliver short, 2 to 4 seconds, 365 nm pulses to individual cells, targeting the nucleus where possible, in order to selectively uncage and activate optPC-Cre in individual cells. After uncaging we transferred the worms to an NGM agar plate without PCK for recovery and to allow for induced Chrimson::mKate2 expression(**Fig. 4c**). After 12-24h we saw strong expression of Chrimson::mKate2 which was easily visible under a dissection fluorescence microscope. As expected, the expression was limited to the cells previously targeted with the laser. Neither laser treatment without previous feeding of PCK, nor feeding of PCK without laser illumination resulted in expression of Chrimson::mKate2 (**Fig. 4d,e,f**).

Optogenetic manipulation of PLM touch sensory neurons

Having achieved targeted expression of Chrimson::mKate2 in either or both neurons of the PLM pair, we then used optical stimulation to test the contributions of these neurons to the touch response. We illuminated animals expressing Chrimson::mKate2 in both PLM neurons ($n \geq 17$) with 617nm light (1.5 mW/mm^2), for 5s, which triggered robust forward movement in an ATR dependent manner (**Fig. 4g** and **Supplementary Video 3, Supplementary Video 4**). Mock treated animals not expressing Chrimson::mKate2 showed no response even in the presence of ATR. (**Supplementary Video 5**)

To interrogate the relative contributions of PLML and PLMR cells to the response individually, we illuminated animals where Chrimson::mKate2 expression was switched on in only one of the two PLM neurons. Groups of animals were illuminated as for both PLMs. Stimulation of either PLML or PLMR alone resulted in a clear response, albeit at slower average velocity compared to the stimulation of both PLMs together**.** Interestingly, stimulation of PLML resulted in a weaker response, compared to stimulation of PLMR as determined by average forward velocity (**Figure 4 g-i, Supplementary Figure 4, Supplementary Videos 6 & 7)**.

When we subjected animals to repeated stimuli of 5 sec illumination every 30 seconds over the course of 3 minutes for a total of 7 stimulations (**Fig. 5**), we observed differences in the response adaptations of each condition. Worms expressing Chrimson::mKate2 in both PLM neurons, continued to respond robustly to stimulation even after several pulses, albeit the response gradually declined in

speed, consistent with habituation to the stimulus **(Fig. 5 a,e,f**, **Supplementary Fig. 5).** The response of worms expressing Chrimson::mKate2 in PLMR only, dropped sharply from the first to the fourth stimulus **(Fig. 5 c,e,f**, **Supplementary Fig. 5)**. In contrast, PLML animals showed steady responses, which were initially weaker than the response for PLMR, but showed no significant reduction after repeated stimulation, apart from a drop from the first to the second stimulus**(Fig. 5 b,e,f, Supplementary Fig. 5).**

Discussion

We have developed a robust and efficient method for the incorporation of ncAAs in *C. elegans*; extensions of this approach will enable a wide range of new chemical functionalities to be introduced into *C. elegans*, including crosslinkers, bioorthgonal groups, and post translational modifications, and this will facilitate many new approaches to manipulating and understanding biology[12,34–39]. We have used our efficient genetic code expansion system to create an optimized photo-activatable Cre recombinase for Laser-TAC. Our photo-activatable Cre has several unique advantages for optical control of gene expression: i) the recombination activity is tightly controlled – the photocaging group completely ablates activity, it is not removed by ambient light, and the photoactivation generates wild-type Cre[13,14], ii) following photoactivation, the photocaged amino acid is withheld and this switches off amber suppression and translation of full length Cre, leaving wild-type worms for subsequent biological studies[40], and iii) due to the stability of the photo-caging group at longer wavelengths, our photoactivatable Cre is fully compatible with imaging and optogenetic methods that use visible light.

We used Laser-TAC to switch on expression of optogenetic channels in a single neuron within a bilaterally symmetric pair that cannot be targeted by genetic means, thereby optically splitting gene expression in anatomically symmetric neurons. Switching on expression of target genes using Laser-TAC is fast and enables the generation of large numbers of animals for downstream experiments. The equipment required for this method is present in most *C. elegans* laboratories as it requires only a microscope-mounted laser generally used for ablation, modified to emit light at 365nm. We demonstrated the utility of the system by subsequently globally illuminating groups of freely moving animals to stimulate the targeted neurons that expressed optogenetic channels. We thereby dissected the individual contributions of two touch sensory neurons, PLMR and PLML to the *C. elegans* touch response.

Our results suggest a model where PLMR is the main driver of the PLM neuronal pair-triggered responses, activating the forward locomotory circuit through activation of the PVCR interneuron via gap junctions, while inhibiting the backward locomotion circuit through inhibitory chemical synapses to the AVA and AVD interneuron pairs.

On the other hand, PLML, activation of which alone results in lower response velocity than for PLMR, may act to amplify the PLMR induced response through activation of PVCL via gap junction coupling.

Interestingly, stimulation of PLMR alone in the absence of additional input from

PLML appears to result in faster habituation compared to the stimulation of both PLMs together. While the response to stimulating PLML alone, even though weaker at first, appears to be steady throughout repeated stimuli, apart from a drop after the first stimulus.

Previous studies addressing functional differences in individual cells in the ASE and AWC neuron pairs have depended on the availability of cell specific promoters, which are only available due to the morphological and developmental asymmetry found within the members of the two pairs stemming from L/R specific sub-differentiation programs. For the vast majority of neuronal pairs in *C. elegans,* cell specific promoters are not available and therefore their functional lateralities have not been addressed. Our approach makes it possible to optically separate cells of morphologically and developmentally symmetric pairs within functional, complete circuits, allowing us to uncover functional asymmetries.

Our method will allow the specific control of gene expression in individual neurons in *C. elegans* irrespective of their position, or the availability of cell specific promoters. While we have focused on expression of optogenetic channels, simple extensions of our approach will enable the cell specific expression of toxins for the inhibition of chemical synapses, or other neuromodulatory proteins. By inserting loxP sites into genomic loci using CRISPR/Cas9, it will be possible to control, at single cell resolution, the expression of any endogenous protein, such as neuropeptides, receptors, innexins, proteins involved in synaptic transmission, etc. We anticipate that these approaches will help to provide insight into the information processing properties of the *C. elegans* nervous system at the single cell level.

Methods

Plasmids

All expression plasmids were generated from pENTR plasmids using Gateway cloning. All plasmids are described in Supplementary Table 1.

C. elegans strains

Strains were maintained under standard conditions unless otherwise indicated[41,42].

Transgenic worms were generated by biolistic bombardment using hygromycin B as a selection marker[43] in either N2 or *smg-2(e2008)* background. Gamma-irradiation to generate the integrated line SGR56 from SGR55 was carried out by Michael Fasseas (Invermis). Integrated lines were backcrossed twice into N2 and subsequently maintained on standard NGM. All non-integrated lines were maintained on NGM supplemented with hygromycin B (0.3 mg/ml) (Formedium). Strains used in this paper are listed in Supplementary Table 2.

Imaging

All imaging was carried out on a Zeiss M2 imager. Worms were mounted on glass slides for imaging and immobilized in a drop of M9 supplemented with 25mM NaN_3.

ncAA feeding

Photo-caged lysine (PCK) was custom synthesized by ChiroBlock GmbH. PCK-NGM plates were prepared by dissolving PCK powder in a small volume of 0.02M HCl and adding the solution to molten NGM. The HCl in the NGM was neutralised by addition of equimolar amounts of NaOH.

Animals were age synchronized by bleaching[42] and added to PCK-NGM plates as L1 larvae. Food was then added to the PCK-NGM plates in the form of solubilized freeze-dried OP50 (LabTIE).

Worm Lysis and Western blotting

Synchronized populations were grown on PCK-NGM plates until the young adult stage and washed off plates using M9 buffer supplemented with 0.001% Triton-X100. Worms were settled, supernatant was removed and worms were resuspended in undiluted 4xLDS loading buffer supplemented with reducing agent (Thermo Fisher Scientific). Lysis was performed by a freeze/thaw cycle followed by 10 minute incubation at 95C.

Samples were run on precast Bolt 4 to 12% gels (ThermoFisher) for 22min at 200V. Proteins were transferred from gel onto a nitrocellulose membrane using an iBlot2 device (ThermoFisher).

After transfer the membrane was blocked in 5% milk powder with PBST (0.1% Tween-20) for 1h at room temperature. Incubation with primary antibodies was carried out in PBST + 5% milk powder at 4C overnight. Blots were washed 6 x 5

minutes with PBST + 5% milk powder before incubating with secondary antibody for 1h at room temperature.

Primary antibodies used: mouse anti-GFP (clones 7.1 and 13.1) (Roche) at a dilution of 1:4000, rat anti-HA clone 3F10 (Roche) at a dilution of 1:2000. Secondary antibodies: Horse anti-mouse IgG HRP (Cell Signaling Technology) at a dilution of 1:5000, Goat anti-Rat IgG (H+L) HRP (Thermo Fisher Scientific) 1:5000. Pierce ECL Western Blotting Substrate (Thermo Scientific) or SuperSignal West Femto chemiluminescent Substrate (Thermo Scientific) were used as detection agent. For quantification of bands a C-Digit Blot Scanner (LI-COR) was used, intensities were analyzed using ImageStudio software.

Global uncaging of PCK for Cre activation

Worms were age synchronized and grown on PCK-NGM plates for 48h, washed onto unseeded 6cm NGM plates and illuminated for 5 min, 5mW/cm^2 in a 365nm CL-1000L crosslinker (UVP). After uncaging worms were transferred to seeded NGM plates and scored for expression of target gene 24h later. 400 μM FUDR was added to plates after uncaging to facilitate counting. All plates were scored blind and counted twice independently by two people. Experiments were performed three times with two independent transgenic lines each. Significance tests were carried out using Welch's t test as a pairwise comparison between each condition at each concentration using Prism8 software.

Uncaging for Cre activation in single neurons

Worms were grown on 4mM PCK from the L1 stage. For uncaging, worms were mounted on a 3% agar and immobilized with 25mM NaN_3 in M9 buffer. Targeting was performed on a Zeiss M2 Imager using an Andor Micropoint module, fitted with a 365nm dye cell. Neurons were identified and targeted using GFP, co-expressed with photo-caged Cre, as a guide. We targeted nuclei were possible. Each region was swept twice using 10 repeat firing. In our settings we set the manual attenuator to full power and the Andor software attenuator to a power of 31 (we chose the power setting so that partial bleaching of GFP could be observed during Micropoint firing). After uncaging, worms were washed off of the pad onto seeded 6cm plates using M9 + 0.001% Triton-X.

Behavioural Assays

Immediately after uncaging, worms were transferred to NGM plates supplemented with ATR (30μl 5mM ATR dissolved in ethanol were added to the lawn of a seeded 6cm NGM plate). Worms were left to recover on ATR plates for 24 hours after laser uncaging.

Plates for behavioural assays were made approximately one hour before use. Fresh 6cm NGM plates were seeded with a 20μl drop of 40X diluted (according to the manufacturer's instructions) LabTIE freeze-dried OP50. The lawn was then surrounded by a copper ring to prevent worms from leaving the camera field of view. Worms with red fluorescence, clearly visible in a Leica fluorescence dissection

scope, in either or both PLM neurons, were picked from the ATR plates onto the behaviour plates. Worms were left to acclimatise on behaviour plates for at least 10 minutes. Behavioural assays were carried out using a WormLab system (MBF Bioscience). Worms were imaged with infrared light and Chrimson was activated using the integrated 617nm red LED of the WormLab at 1.5mW/mm^2.

Tracking of worm behaviour was carried out using WormLab software (MBF Bioscience). For each worm, tracks detected by the WormLab software were consolidated into a single track. For statistical analyses raw speed data for each worm was binned and averaged at 1s intervals. Fisher's exact test and Mann-Whitney u-test statistics were performed using Prism8 software.

Acknowledgements:

We thank Maria Doitsidou, Emanuel Busch, and Kathrin Lang for helpful suggestions and input on the manuscript, and Zoltan Soltesz for help with initial experiments.

We thank the European Research Council (ERC-StG-679990), the Wellcome-Trust University of Edinburgh Institutional Strategic Support Fund ISS2, the Royal Society, and the Muir Maxwell Epilepsy Centre for funding to S.G., the University of Edinburgh for a Edinburgh Global Award and Principal's Career Development PhD studentship to Z.X.; we thank the MRC (MC_U105181009 and MC_UP_A024_1008) and the Louis Jeantet Foundation for funding to J.W.C.; I.R. thanks the Herchel Smith Foundation for a studentship.

Some strains were provided by the Caenorhabditis Genetics Centre for strains, funded by NIH Office of Research Infrastructure Programs (P40OD010440)

References

1. White, J. G., Southgate, E., Thomson, J. N. & Brenner, S. The structure of the nervous system of the nematode Caenorhabditis elegans. *Philos. Trans. R. Soc. Lond. B. Biol. Sci.* **314**, 1–340 (1986).
2. Troemel, E. R., Sagasti, A. & Bargmann, C. I. Lateral signaling mediated by axon contact and calcium entry regulates asymmetric odorant receptor expression in C. elegans. *Cell* **99**, 387–398 (1999).
3. Wes, P. D. & Bargmann, C. I. C. elegans odour discrimination requires asymmetric diversity in olfactory neurons. *Nature* **410**, 698–701 (2001).
4. Suzuki, H. *et al.* Functional asymmetry in Caenorhabditis elegans taste neurons and its computational role in chemotaxis. *Nature* **454**, 114–117 (2008).
5. Hobert, O., Johnston, R. J. & Chang, S. Left-right asymmetry in the nervous system: the Caenorhabditis elegans model. *Nat. Rev. Neurosci.* **3**, 629–640 (2002).
6. Leifer, A. M., Fang-Yen, C., Gershow, M., Alkema, M. J. & Samuel, A. D. T. Optogenetic manipulation of neural activity in freely moving Caenorhabditis elegans. *Nat. Methods* **8**, 147–152 (2011).

7. Stirman, J. N. *et al.* Real-time multimodal optical control of neurons and muscles in freely behaving Caenorhabditis elegans. *Nat. Methods* **8**, 153–158 (2011).
8. Churgin, M. A., He, L., Murray, J. I. & Fang-Yen, C. Efficient single-cell transgene induction in Caenorhabditis elegans using a pulsed infrared laser. *G3 (Bethesda).* **3**, 1827–1832 (2013).
9. Bacaj, T. & Shaham, S. Temporal control of cell-specific transgene expression in Caenorhabditis elegans. *Genetics* **176**, 2651–2655 (2007).
10. Schindler, S. E. *et al.* Photo-activatable Cre recombinase regulates gene expression in vivo. *Sci. Rep.* 1–8 (2015).
11. Kawano, F., Okazaki, R., Yazawa, M. & Sato, M. A photoactivatable Cre-loxP recombination system for optogenetic genome engineering. *Nat. Chem. Biol.* **12**, 1059–1064 (2016).
12. Chin, J. W. Expanding and reprogramming the genetic code. *Nature* **550**, 53–60 (2017).
13. Luo, J. *et al.* Genetically encoded optical activation of DNA recombination in human cells. *Chem. Commun.* **52**, 8529–8532 (2016).
14. Brown, W., Liu, J., Tsang, M. & Deiters, A. Cell-Lineage Tracing in Zebrafish Embryos with an Expanded Genetic Code. *Chembiochem* **19**, 1244–1249 (2018).
15. Greiss, S. & Chin, J. W. Expanding the Genetic Code of an Animal. *J. Am. Chem. Soc.* **133**, 14196–14199 (2011).
16. Nikić, I. *et al.* Debugging Eukaryotic Genetic Code Expansion for Site-Specific Click-PAINT Super-Resolution Microscopy. *Angew. Chemie Int. Ed.* **55**, 16172–16176 (2016).
17. Gautier, A. *et al.* Genetically encoded photocontrol of protein localization in mammalian cells. *J. Am. Chem. Soc.* **132**, 4086–4088 (2010).
18. Yochem, J., Gu, T. & Han, M. A new marker for mosaic analysis in Caenorhabditis elegans indicates a fusion between hyp6 and hyp7, two major components of the hypodermis. *Genetics* **149**, 1323–1334 (1998).
19. Parrish, A. R. *et al.* Expanding the Genetic Code of Caenorhabditis elegans Using Bacterial Aminoacyl-tRNA Synthetase/tRNA Pairs. *ACS Chem. Biol.* (2012).
20. Yumerefendi, H. *et al.* Control of Protein Activity and Cell Fate Specification via Light-Mediated Nuclear Translocation. *PLoS One* **10**, e0128443-19 (2015).
21. Serfling, R. *et al.* Designer tRNAs for efficient incorporation of non-canonical amino acids by the pyrrolysine system in mammalian cells. *Nucleic Acids Res.* **46**, 1–10 (2018).
22. Gibb, B. *et al.* Requirements for catalysis in the Cre recombinase active site. *Nucleic Acids Res.* **38**, 5817–5832 (2010).
23. Le, Y., Gagneten, S., Tombaccini, D., Bethke, B. & Sauer, B. Nuclear targeting determinants of the phage P1 cre DNA recombinase. *Nucleic Acids Res.* **27**, 4703–4709 (1999).
24. Macosko, E. Z. *et al.* A hub-and-spoke circuit drives pheromone attraction and social behaviour in C. elegans. *Nature* **458**, 1171–1175 (2009).
25. Maricq, A. V., Peckol, E., Driscoll, M. & Bargmann, C. I. Mechanosensory signalling in C. Elegans mediated by the GLR-1 glutamate receptor. *Nature* **378**, 78–81 (1995).

26. Guo, F., Gopaul, D. N. & van Duyne, G. D. Structure of Cre recombinase complexed with DNA in a site-specific recombination synapse. *Nature* **389**, 40–46 (1997).
27. Lyssenko, N. N., Hanna-Rose, W. & Schlegel, R. A. Cognate putative nuclear localization signal effects strong nuclear localization of a GFP reporter and facilitates gene expression studies in Caenorhabditis elegans. *Biotechniques* **43**, 560,596,598 (2007).
28. Schultheis, C., Brauner, M., Liewald, J. F. & Gottschalk, A. Optogenetic analysis of GABAB receptor signaling in Caenorhabditis elegans motor neurons. *J. Neurophysiol.* **106**, 817–827 (2011).
29. Chalfie, M. *et al.* The neural circuit for touch sensitivity in Caenorhabditis elegans. *J. Neurosci.* **5**, 956–964 (1985).
30. Schild, L. C. & Glauser, D. A. Dual color neural activation and behavior control with chrimson and CoChR in Caenorhabditis elegans. *Genetics* **200**, 1029–1034 (2015).
31. Wicks, S. R. & Rankin, C. H. Integration of mechanosensory stimuli in Caenorhabditis elegans. *J. Neurosci.* **15**, 2434–2444 (1995).
32. Mitani, S., Du, H., Hall, D., Driscoll, M. & Chalfie, M. Combinatorial control of touch receptor neuron expression in Caenorhabditis elegans. *Development* **119**, 773–783 (1993).
33. Arellano-Carbajal, F. *et al.* Macoilin, a conserved nervous system-specific ER membrane protein that regulates neuronal excitability. *PLoS Genet.* **7**, (2011).
34. Davis, L. & Chin, J. W. Designer proteins: applications of genetic code expansion in cell biology. *Nat. Rev. Mol. cell Biol.* **13**, 168–182 (2012).
35. Nguyen, T. A., Cigler, M. & Lang, K. Expanding the Genetic Code to Study Protein–Protein Interactions. *Angew. Chemie - Int. Ed.* **57**, 14350–14361 (2018).
36. Lang, K. & Chin, J. W. Cellular incorporation of unnatural amino acids and bioorthogonal labeling of proteins. *Chem. Rev.* **114**, 4764–4806 (2014).
37. Young, D. D. & Schultz, P. G. Playing with the Molecules of Life. *ACS Chem. Biol.* **13**, 854–870 (2018).
38. Zhang, G., Zheng, S., Liu, H. & Chen, P. R. Illuminating biological processes through site-specific protein labeling. *Chem. Soc. Rev.* **44**, 3405–3417 (2015).
39. Baker, A. S. & Deiters, A. Optical control of protein function through unnatural amino acid mutagenesis and other optogenetic approaches. *ACS Chem. Biol.* **9**, 1398–1407 (2014).
40. Maywood, E. S. *et al.* Translational switching of Cry1 protein expression confers reversible control of circadian behavior in arrhythmic Cry-deficient mice. *Proc. Natl. Acad. Sci. U. S. A.* **115**, E12388–E12397 (2018).
41. Brenner, S. The genetics of Caenorhabditis elegans. *Genetics* **77**, 71–94 (1974).
42. Stiernagle, T. Maintenance of C. elegans. *WormBook* 1–11 (2006).
43. Radman, I., Greiss, S. & Chin, J. W. Efficient and Rapid C. elegans Transgenesis by Bombardment and Hygromycin B Selection. *PLoS One* **8**, e76019 (2013).

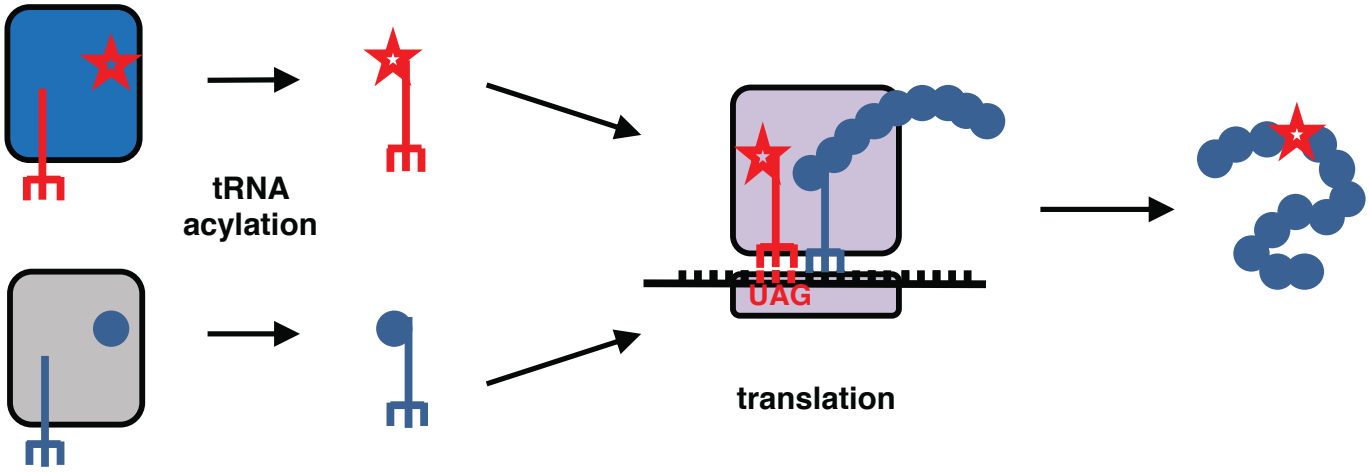

Figure 1 Genetic code expansion. An unnatural amino acid (red star) is charged onto an orthogonal $tRNA_{CUA}$ (red trident) by an orthogonal tRNA-synthetase (top left, blue). The orthogonal components do not interact with the native cellular amino acids (blue circle), tRNAs (blue trident) or tRNA-synthetases (bottom left, grey). After charging, the ncAA-$tRNA_{CUA}$ can be incorporated into an expanding polypeptide chain in response to an amber stop codon (TAG) during ribosomal translation (centre). The resultant polypeptide is released following translation resulting in full-length protein containing the ncAA residue (right).

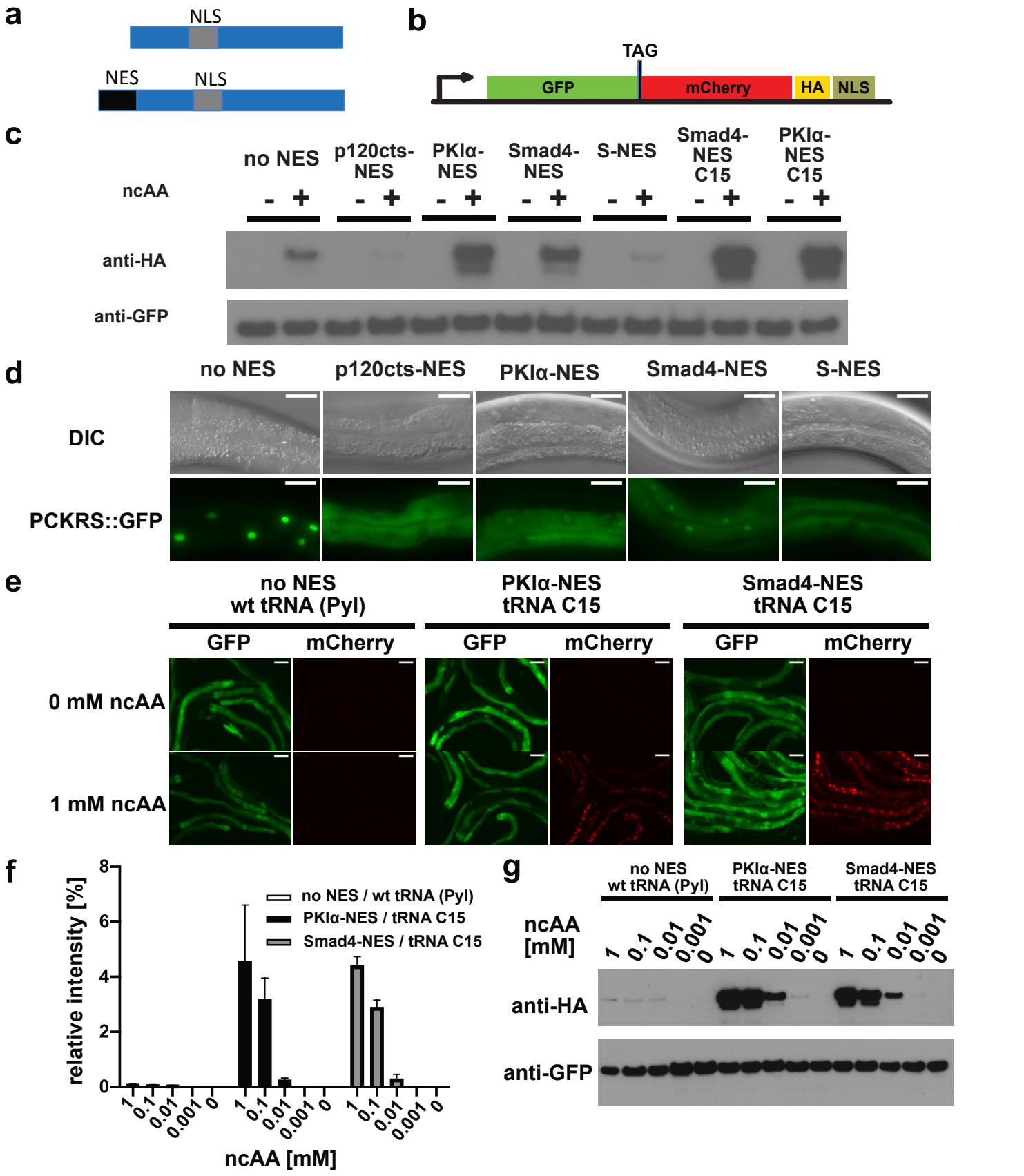

Figure 2. Efficiency of genetic code expansion is enhanced in *C. elegans* by use of NES-PCKRS and tRNA(C15). (**a**) wild type PylRS/PCKRS (top) contains an internal nuclear localization sequence (NLS) which targets it to the nucleus. A strong nuclear export sequence (NES) can be added to PylRS/PCKRS to shift it to the cytoplasm (bottom). (**b**) The GFP::mCherry reporter has an intersubunit linker containing an amber stop codon (TAG) to direct incorporation of ncAA. The C-terminal NLS moves full length product to the nucleus, providing a second visual readout, whilst the C-terminal HA tag provides a target for Western blotting of full-length protein. (**c**) Western blot comparison of total (anti-GFP) vs full-length (anti-HA) reporter produced using PCKRS with different NES attached to the N-terminus, co-expressed with wild type $tRNA(Pyl)_{CUA}$; Smad-4 and PKIα NES-PCKRS with tRNA(C15). ncAA + or – indicates the respective presence or absence of 1mM ncAA. (**d**) Nuclear localization of NES variants fused to PCKRS. Localization visualized by imaging of a GFP protein directly fused to each PCKRS. scale bars 30 µm (**e**) Fluorescent imaging of worms grown in the presence or absence of 1mM ncAA. GFP indicates expression of reporter construct, mCherry indicates presence of full-length reporter protein. Scale bars 30 µm (**f**) Relative quantification of Western blots of no NES PCKRS vs both PKIα and Smad-4 NES-PCKRS at different ncAA concentrations; relative intensities of the GFP signal of the full length product vs GFP signal of the product truncated at the amber stop codon (g) Samples shown in (f) probed with anti-HA and anti-GFP.

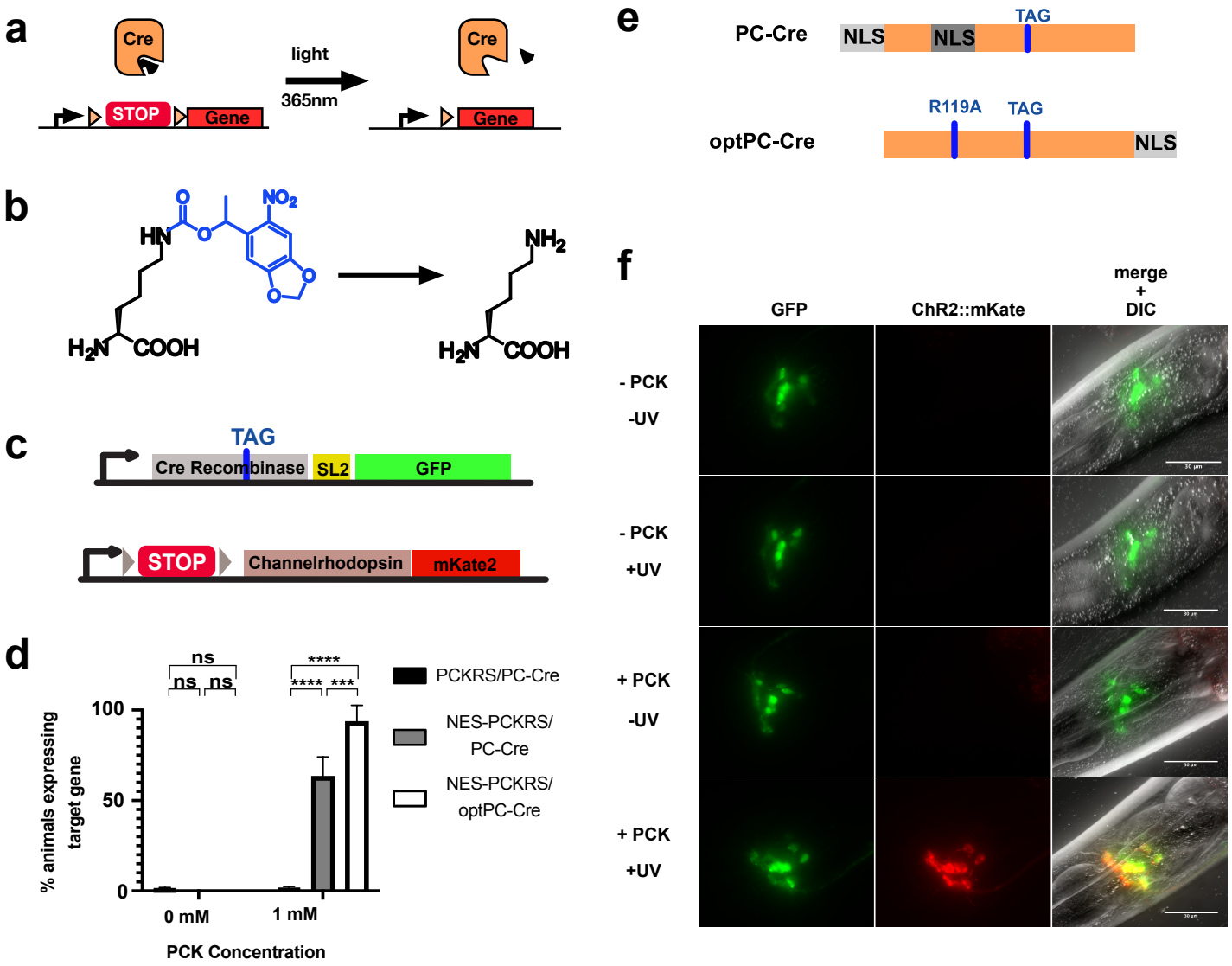

Figure 3 Optimisation of PC-Cre recombinase for genetic code expansion in *C. elegans*. (**a**) Cre recombinase can by photocaged by incorporating a photo-caged ncAA into the active site (black wedge). Transcription of target gene is blocked by placing a transcription stop sequence between the gene and its promoter. The stop sequence is flanked by loxP sites (orange triangles). Upon illumination at 365nm the photo-caging group is removed and the uncaged Cre removes the transcription stop sequence. (**b**) 6-nitropiperonyl-L-Lysine, "photo-caged lysine" (PCK) is a lysine residue with a 2-nitrobenzyl derived photo-caging group on the side chain. The photo-caging group is removed at 365nm. (**c**) Genetic constructs for PC-Cre controlled expression of channelrhodopsin. (**d**) Cre activation efficiency in animals with optimised vs original constructs. Comparison of original PCKRS and *M. mazei* tRNA(Pyl)$_{CUA}$ ("PCKRS"), modified NES-PCKRS and tRNA(C15) ("NES-PCKRS"), original photocaged Cre recombinase ("PC-Cre") and optimized photo-caged Cre ("optPC-Cre"). Significance derived from P values of Welch's t test. The error is the standard deviation. (**e**) Schematic showing PC-Cre and optPC-Cre. Substitution mutations shown as blue bars. TAG mutation facilitates PCK incorporation. PC-Cre contains both an N-terminal and internal NLS. OptPC-Cre contains only a C-terminal NLS, the R119A mutation disables the internal NLS. (**f**) Imaging of worms bombarded with Smad4 NES-PCKRS, tRNA(C15) and optPC-Cre. Expression of ChR2::mKate2 is dependent on supplementation of PCK and uncaging by exposure to UV light.

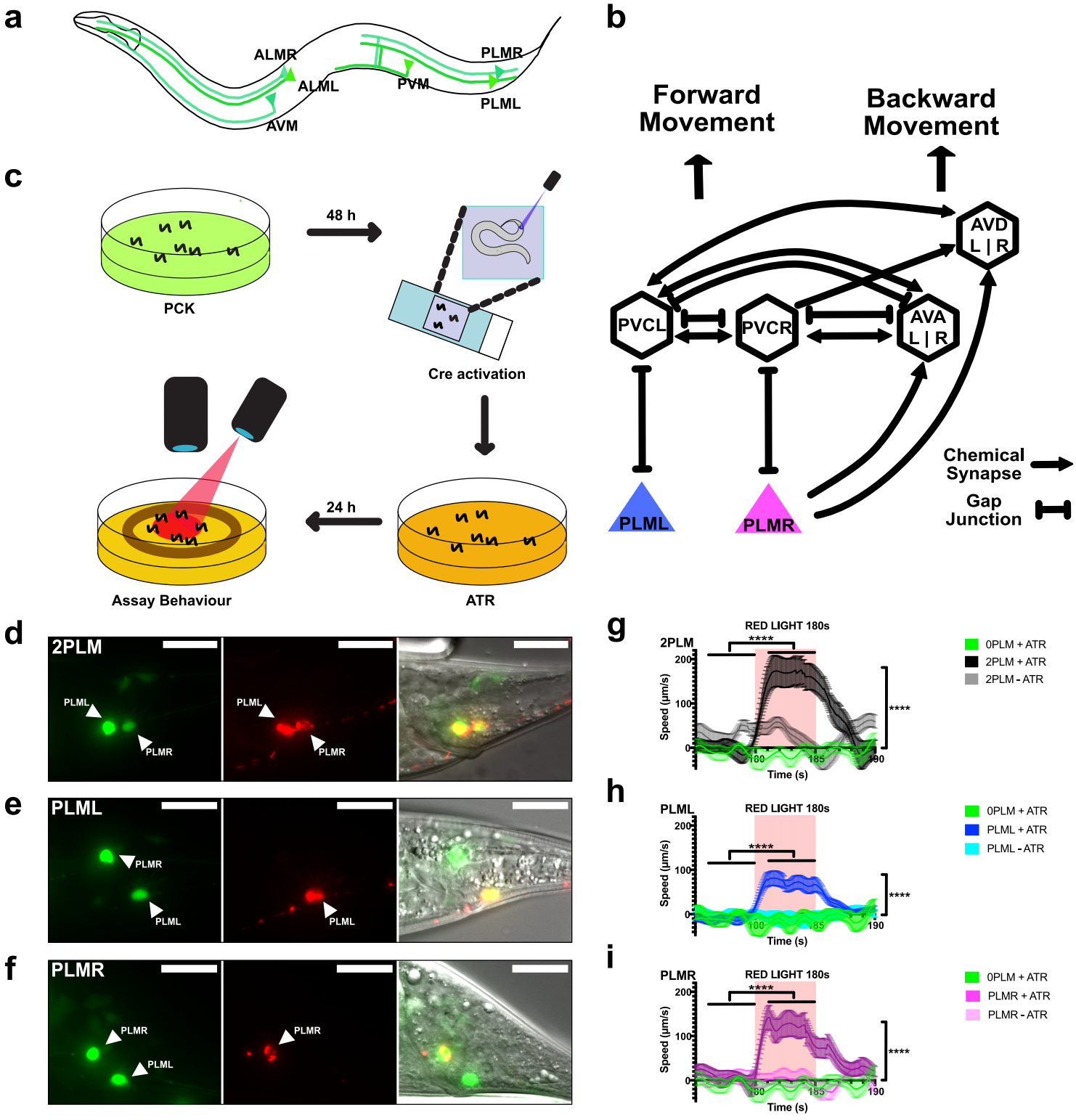

Figure 4 Laser-TAC using optimised Photocaged Cre-recombinase facilitates cell-specific expression of optogenetic channels in *C. elegans*. **(a)** Map of the six *C. elegans* touch receptor neurons showing the PLM neuronal pair located at the posterior of the worm. **(b)**. Simplified schematic of the asymmetric neuronal connectivity of PLML and PLMR within the touch circuit. **(c)** Diagram of experimental procedure for activating expression of target genes in single cells using Laser-TAC. **(d**,**e** and **f)**. Fluorescent images showing targeted expression of Chrimson::mKate2 24h after Laser induced activation of optPC-Cre (middle panels) in both PLM neurons (**d**), only in PLML (**e**), only in PLMR (**f**). Scale bars 20µm. GFP signal indicates cells expressing optPC-Cre (left panels). **(g**, **h** and **i)** Average speed curves of each condition in response to a single 5 second pulse of red light. Curves correspond to expression of Chrimson channel in both PLMs (**g**, black), PLML alone (**h**, blue) or PLMR alone (**i**, magenta). -ATR control curves are shown in paler colours. Controls grown on ATR, but without optPC-Cre activation and not expressing Chrimson (0PLM + ATR) are shown in green on each chart. For 0PLM +ATR control n=10, for all others n≥12. Horizontal black bars mark significance of P values derived from Mann-Whitney U test comparisons of uncaged worms on ATR between the areas indicated. Vertical bars represent the significance of P values between conditions from a mixed model analysis between all 3 condition on each graph. All error bars represent the standard error from the mean.

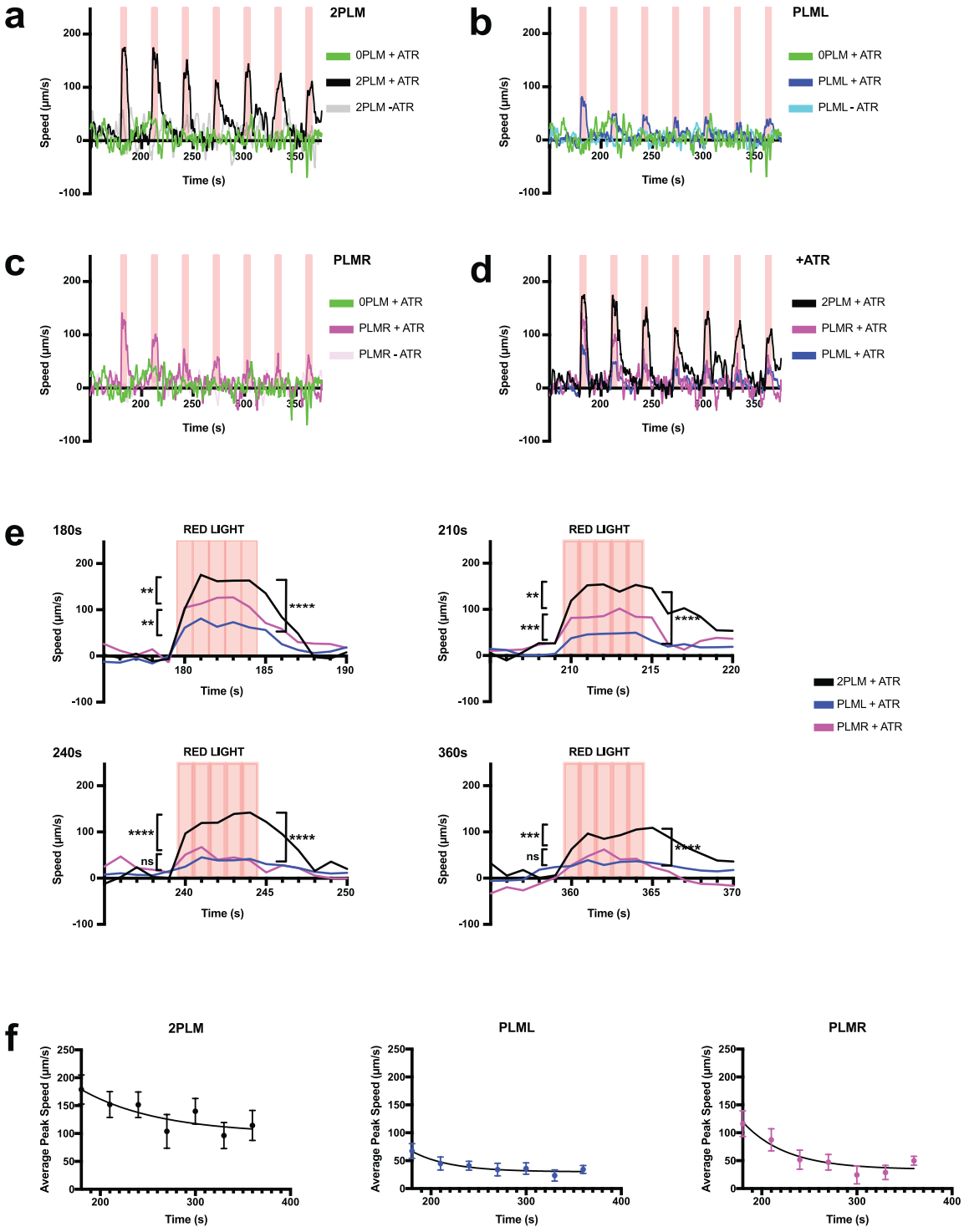

Figure 5 PLM neurons show distinct responses to repeat optogenetic stimulation. **(a-c)** Average smoothed speed responses over multiple stimulations (5s, 1.5 mW/cm^2, 617 nm) for both PLM neurons ("2PLM") (**a**), PLML alone (**b**), PLMR alone (**c**). Red vertical lines indicate when illumination is switched on. "0PLM' indicates mock treated animals not expressing optogenetic channel. For 0PLM + ATR, n = 10, for all other conditions n. **(d)** All speed responses shown in (a-c) combined. **(e)** Comparison of 2PLM (black), PLML (blue) and PLMR (magenta) speeds averaged per second in response to the first three stimuli, and the last stimulus. All significances derived from P values obtained by Mann-Whitney U test comparisons between conditions. upper left significance: 2PLM vs PLMR; lower left: PLMR v PLML; right: 2PLM v PLML. n **(f)** Average speeds during repeated 5s stimulation for 2PLM (black), PLML (blue) or PLMR (magenta). The error is the standard error from the mean. All responses fitted to an exponential decay using least-squares fit.